

Probing the Nature of the Blue-Shifted Intermediate of Photoactive Yellow Protein in Solution by NMR: Hydrogen–Deuterium Exchange Data and pH Studies[†]

C. Jeremy Craven,^{‡,§,||} Nocky M. Derix,^{‡,||} Johnny Hendriks,[‡] Rolf Boelens,[‡] Klaas J. Hellingwerf,[‡] and Robert Kaptein^{*,‡}

Department of NMR Spectroscopy, Bijvoet Center for Biomolecular Research, Utrecht University, Padualaan 8, 3584 CH Utrecht, The Netherlands, and Department of Microbiology, E. C. Slater Instituut, BioCentrum Amsterdam, University of Amsterdam, Nieuwe Achtergracht 127, 1018 WS Amsterdam, The Netherlands

Received July 12, 2000; Revised Manuscript Received August 24, 2000

ABSTRACT: The nature of the pB intermediate of photoactive yellow protein (PYP) from *Ectothiorhodospira halophila* has been probed by NMR. pH-dependent changes in the NMR spectrum of the dark state of PYP are shown to closely mimic exchange broadening effects observed previously in the NMR spectrum of the pB intermediate in solution. Amide H–D exchange data show that while pB retains a solid protected core, two regions become significantly less protected than the dark state. The amide exchange data help to rationalize why the conformational exchange process affects the N-terminal 28-residue segment of the protein, which is not close to the site of chromophore rearrangement. At very low pH (pH 1.7), the dark state NMR spectrum displays approximately 30 very sharp signals, which are characteristic of a portion of the molecule becoming unfolded. Similarities between the dark state spectra at pH ~3.2 and the spectra of pB suggest a model for pB in solution where the protein exists in an equilibrium between a well-ordered state and a state in which a region is unfolded. Such a two-state model accounts for the exchange phenomena observed in the NMR spectra of pB, and the hydrophobic exposure and lability inferred from thermodynamic data. It is likely that in the crystalline environment the ordered form of pB is strongly favored.

The nature of the various states that the photoactive yellow protein (PYP)¹ from *Ectothiorhodospira halophila* populates during its photocycle has attracted much study (1–18). Although definite genetic proof is still lacking, the available evidence indicates that the photoactive behavior of the protein is involved in the control of the negative phototactic response of *E. halophila* to blue light. More generally, PYP, which is highly water soluble and crystallizable, provides a very useful experimental model for understanding the photocycle of other photoactive proteins, many of which are membrane-bound.

During the photocycle of PYP, the molecule passes through several distinct states, some of which are populated very rapidly after light absorption, and only very transiently. These states are accessible to study by time-resolved X-ray crystallography (7, 17), and such studies have shown that they involve small changes which occur very locally within

the chromophore region after light absorption, after which a more marked rearrangement occurs to produce the so-called pB intermediate, which is characterized spectroscopically by a blue-shifted absorption maximum. The pB state, which is reached in less than a millisecond after light absorption, remains stable on the subsecond time scale, returning to the ground state pG at a rate that is very pH sensitive. X-ray crystallography (2) indicates that the key change which occurs in the structure upon the formation of pB is the conversion of the vinyl bond of the *p*-coumaric acid chromophore from a trans to a cis conformation. This rotates the phenolic moiety out of the pocket into which it is bound in pG, exposing the phenolic oxygen to the solvent. In pG, the phenolic group is deprotonated and stabilized by a network of hydrogen bonds to the protein, whereas in pB, it is solvent-exposed and thus protonated. This change in protonation state is responsible for the change of the absorption maximum of the conjugated system.

Due to the short time scales involved, the short-lived states of PYP are not amenable to study by NMR. The pB intermediate, however, is sufficiently long-lived to be studied by NMR (4), and many of the necessary techniques have been described elsewhere (19). In brief, they require laser excitation of the PYP molecule directly in the NMR tube before the acquisition of each scan of a one-dimensional or two-dimensional experiment. Furthermore, it is possible to assign the signals in the ¹⁵N HSQC spectra of pB by generating spectra containing exchange cross-peaks (SCOTCH experiment).

[†] Financial support from the Netherlands Foundation for Scientific Research (NWO-CW) is gratefully acknowledged.

* Corresponding author. E-mail: kaptein@nmr.chem.uu.nl.

[‡] University of Utrecht.

[§] On leave from Krebs Institute for Biomolecular Research, Department of Molecular Biology and Biotechnology, University of Sheffield, Firth Court, Western Bank, Sheffield S10 2TN, U.K.

^{||} These authors contributed equally to this work.

¹ University of Amsterdam.

¹ Abbreviations: H–D, hydrogen–deuterium; HSQC, heteronuclear single-quantum coherence spectroscopy; NMR, nuclear magnetic resonance; pG, ground state of the PYP photocycle; pB, blue-shifted intermediate of the PYP photocycle; pB_{dark}, low-pH form of PYP in the dark; pB_{punf}, partially unfolded form of pB; pB_{xtl}, structured form of pB as determined by X-ray crystallography; PYP, photoactive yellow protein.

By X-ray crystallography, the pB state appears to be well-described by a single structure (2). In this structure, the only major change compared to pG is in the conformation of the chromophore as described above, along with some minor rearrangements of the protein packing around the chromophore. In solution, however, a quite different picture is revealed by NMR (4). In particular, the spectra of pB are not consistent with a single well-ordered state, since many of the expected cross-peaks in the ^{15}N HSQC spectra are not present, indicating that there is significant conformational exchange occurring on the millisecond time scale. The broadening of the spectra of pB due to this exchange process has thus far precluded more detailed structural conclusions. As we highlight in this paper, one particularly intriguing feature is that although some parts of the protein that are involved in the conformational exchange process are near the chromophore, the N-terminal 28 residues of PYP, which are quite distant from the chromophore, also appear to be involved. Thus, it appears that to conclude from the X-ray structure that the only significant change is around the site of the chromophore itself is not an adequate description of the changes that occur upon formation of pB in solution. Further complexity in PYP arises from analysis of the dependence of the pB \rightarrow pG recovery process on temperature and denaturant concentration (1, 3, 18), which shows that the formation of pB involves the exposure of a large area of hydrophobic surface. It has thus been suggested (3) that the pB state is partially unfolded.

The rate of the pB \rightarrow pG recovery process is strongly pH-dependent, becoming much slower as the pH is lowered (9). This is consistent with the key role of deprotonation of the phenolic group, which must occur at some stage during the return to pG. In the dark, between pH 4 and 1.5 a transition occurs to a state that has properties very similar (but not identical) to those of pB even in the absence of illumination, and has been termed pB_{dark} (9).

To elucidate further the nature of pB, we present here the results of an amide H–D exchange experiment and of a ^{15}N HSQC-monitored pH titration of pG. The H–D exchange experiment allows us to probe the changes in stability of individual hydrogen bonds within the structure upon formation of pB. Since the H–D exchange was monitored by ^{15}N HSQC spectra of the pG state, this experiment is not compromised by the conformational exchange broadening observed in the spectra of pB.

The pH titration of pG allows us to investigate further the nature of the exchange broadening process observed in pB, since we show that a similar effect is observed as the pH is lowered. The amide H–D exchange data show that on formation of pB a local loss of stability occurs in the region of the protein to which the chromophore is hydrogen bonded in pG. This provides an explanation of why the conformational exchange process propagates through such a large region of the protein, including the N-terminal 28-residue segment. The pH data suggest a model for pB in solution as a two-state equilibrium between a well-folded form and a form in which a portion of the molecule is unfolded and highly mobile. Such a model is able to unify the results of NMR, X-ray diffraction, and thermodynamic studies of pB.

MATERIALS AND METHODS

Uniformly ^{15}N -labeled PYP was expressed and purified as described previously (20). Samples contained 50 mM deuterated acetate buffer, and a protease inhibitor cocktail (1 mM pepablock, 5 μM leupepsin, and 1 mM EDTA). All spectra were acquired at 311 K on a Varian UnityPlus 500 spectrometer, with modifications for laser illumination as described previously (19). ^{15}N HSQC spectra were acquired with gradient coherence selection, water flip-back, and sensitivity enhancement (21). Spectra were processed with either NMRPipe (22) or Felix (Molecular Simulations Inc.). All spectra were analyzed in Felix, from which cross-peak intensity data (measured as peak height) were exported for further manipulation using in-house software. The pH titration series was followed in Felix using a suite of macros written in-house.

In the amide H–D exchange experiments, a sample of uniformly ^{15}N -labeled PYP was divided into two equal volumes and lyophilized. Immediately prior to NMR data collection for each experiment, one of the samples was redissolved in D_2O to a concentration of 750 μM , the pH measured (pH 6.1 for both samples), and the sample transferred to a Shigemi NMR tube with a light guide attached to enable laser illumination. Data acquisition commenced within 20 min of dissolution. For the laser illumination experiments, the sequence of data acquisition and illumination was as follows: (i) HSQC acquisition, (ii) HSQC acquisition, (iii) laser illumination over a total time of 4.3 min, (iv) HSQC acquisition, (v) HSQC acquisition, (vi) laser illumination over a total time of 18 min, (vii) HSQC acquisition, (viii) HSQC acquisition, (ix) laser illumination over a total time of 82 min, (x) HSQC acquisition, and (xi) HSQC acquisition. For the dark series of experiments, HSQC spectra were acquired 0, 10, 20, 46, 88, and 150 min after the commencement of acquisition of the first spectrum, and then at times up to 55 h to allow determination of the decay rate of slowly exchanging residues. All HSQC spectra were acquired with acquisition times of 73 (^1H) and 35 ms (^{15}N), with four transients collected, resulting in a total measuring time of 10 min per spectrum. The laser illumination consisted of a series of 0.5 s bursts, repeated every 8 s. This is a level of illumination similar to that used in earlier experiments, for which it was determined that the temperature change induced in the sample was less than 1 K. This repetition rate corresponds to total light exposure times during the three illumination periods of 16, 68, and 308 s. As the conversion to and recovery of pB is rapid at this pH, the period spent in the pB state was taken to be equal to the illumination period without further correction. The data were analyzed by first fitting an exponential decay to the dark series data, using in-house software employing the Marquadt nonlinear least-squares fitting algorithm (23). H–D exchange rates were converted to protection factors using data from Bai et al. (24), with due compensation for the glass electrode effect in D_2O . Curves were then generated which corresponded to the curves that would be obtained in the light experiment if the H–D exchange rate in pB were accelerated over that in pG by factors of 10 – 10^4 , the calculation taking due account of the time that the molecules are in the pB or pG state. These were compared with the actual experimental data to estimate the changes in protection that occur in the pB state.

In cases where the light and the dark state data were indistinguishable within error, this allowed an upper estimate to be placed on the change in protection in pB.

For the pH titration series, the concentration of the protein dissolved in a 90% H₂O/10% D₂O mixture was 1 mM, and the initial sample volume was 500 μ L. The pH was adjusted by addition of microliter quantities of HCl or NaOH. The sample length was used to monitor sample losses, and the cross-peak heights were corrected for dilution effects. ¹⁵N HSQC spectra were acquired with acquisition times of 73 (¹H) and 108 ms (¹⁵N), with a total measuring time of approximately 1 h.

RESULTS

Amide H–D Exchange Experiments. The protection against amide H–D exchange in the pB state was probed by first performing a conventional amide H–D exchange experiment on the pG state, monitored by a series of ¹⁵N HSQC spectra. A second H–D exchange experiment was then performed with a duplicate sample, in which the HSQC spectra were interspersed with periods of laser illumination. In this experiment, the decay of cross-peak intensity was a combination of H–D exchange during the time the protein was in the pB state and of H–D exchange during the time the protein was in the pG state. The HSQC spectra were still acquired in the pG state so that high spectral resolution could be obtained. We refer to these two sets of HSQC spectra as “dark” and “light” experiments, respectively. The details of these experiments are given in Materials and Methods.

In such a pair of experiments, a difference in the protection of a residue against amide H–D exchange in the pB state relative to the pG state will be manifested by a change in the decay rate of the cross-peaks in the two experiments as a function of the total elapsed time after addition of D₂O. Example comparisons of data from the two experiments are shown in Figure 1. Data are shown for two contrasting types of behavior. For residues G29 and T70, a distinct increase in the rate of H–D exchange is observed in the light experiment. In contrast, for residues F75 and V105, no such increase can be detected. By comparison of such plots with plots calculated for varying changes in protection in pB relative to pG, distinct decreases in the level of protection were quantifiable for 14 residues (Figure 2, partly black bars). For the remaining 37 residues for which decay was sufficiently slow in the dark experiment to allow analysis, no detectable difference in decay rate was apparent. For these residues, it was possible to estimate the maximum change in the H–D exchange rate between pB and pG, consistent with the data, so that it was possible to make the statement that the change in the level of protection could be no greater than a certain amount (Figure 2, partly hatched bars).

pH Titration. A series of one-dimensional ¹H spectra and two-dimensional ¹⁵N HSQC spectra of PYP were acquired over the pH range of 5.7–2.1. Chemical shift changes and broadening effects indicate that the pH dependence in this range could be divided into two distinct events. The changes in the upfield region of the one-dimensional ¹H NMR spectrum of PYP are shown in Figure 3. The peak from V83 H² was the mostly strongly affected in the pH range of 5.7–4.2, whereas the other three signals (V57 H², V105 H², and A67 H ^{β}) exhibited small shift or intensity changes in

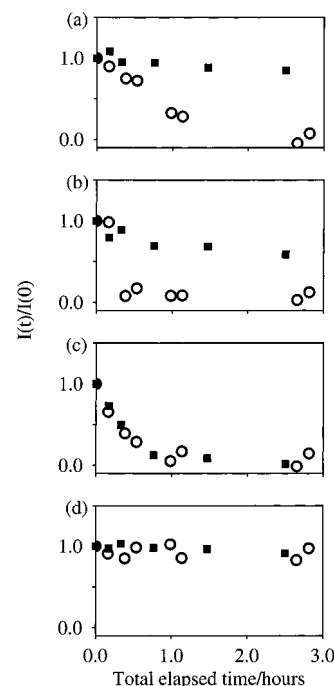


FIGURE 1: Representative amide H–D exchange for four residues. Data are shown for the dark experiment (■) and the light experiment (○). From top to bottom, the data are for (a) G29 and (b) T70, where the H–D exchange is markedly different in the pB state, and for (c) F75 and (d) V105, where it is indistinguishable from that of pG.

this region. At pH <4.2, in contrast, these three signals are markedly broadened, whereas the movement of V83 H² appeared to saturate at pH \sim 3.6. In the ¹⁵N HSQC spectra, many of the cross-peaks that were still detectable at pH <3.6 (see below) showed a distinct change in the direction of movement at this point. For instance, the effect was particularly clear for the side chain amine group of W119 (Figure 3b).

The intensity of backbone amide ¹⁵N HSQC cross-peaks (Figure 4) showed the most intriguing effects, especially in the lower of these two pH ranges. In the pH range of 5.7–4.2, the most significant change in intensity occurred for the cross-peak of residue E12 which became undetectably weak at pH 5.1, with an apparently related drop in intensity of the cross-peak of I11 around the same pH. If it is assumed that this behavior relates to the ionization of the side chain of E12, these data suggest a rather elevated pK for E12, which most likely reflects the acidic nature of the sequence E9–D10–I11–E12. These changes in intensity occurred in relative isolation, with only small changes in intensity for other cross-peaks in the spectrum.

At pH <4.2, intensity changes occurred in the spectrum for many more residues of the protein. The intensity of many cross-peaks started to decrease, indicating the onset of a second transition. By pH 3.2, the HSQC cross-peaks corresponding to approximately half of the residues in the protein had diminished in peak height to an undetectably low level. Fewer than 10 new cross-peaks could be detected; thus, for the majority of the affected resonances, the cross-peak must have become severely exchange broadened. In contrast, and as discussed further below, cross-peaks for residues comprising a significant portion of the molecule retained substantial intensity. This differential effect eliminates the possibility

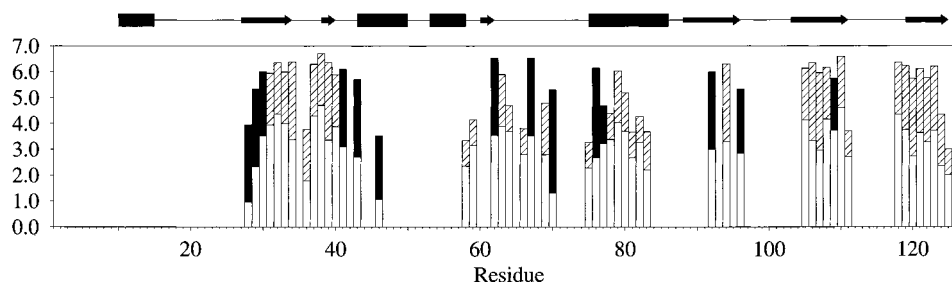


FIGURE 2: Protection factors for backbone amide NH groups in pG and pB. The full height of each bar represents the value for pG. Where the upper part of the bar is shaded black, a distinct difference in the H–D exchange rate could be detected between pG and pB. The black part of the bar represents the change in the protection factor between pG and pB, and thus, the white part of the bar represents the value for pB. Where the upper part of the bar is hatched, no change in the H–D exchange rate could be detected and the upper part of the bar represents the maximum change consistent with the data so that the white part of the bar is the minimum level of protection in pB consistent with the data. The secondary structure of PYP in solution, as defined in D \ddot{u} x et al. (20), is shown above the figure.

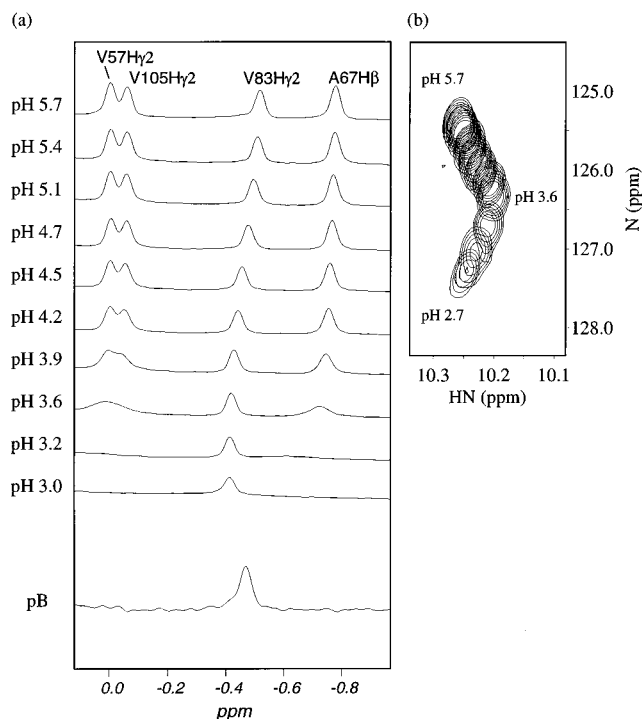


FIGURE 3: Behavior when the pH is lowered can be divided into two distinct events. (a) The upper part of the figure shows the upfield methyl region of the one-dimensional spectrum of pG with decreasing pH. The lower trace shows the equivalent portion of the spectrum of pB. At pH 5.7, the signals are assigned (from left to right) as V57 H γ ², V105 H γ ², V83 H γ ², and A67 H β . (b) A section of the ¹⁵N HSQC spectrum of pG during the pH titration. The cross-peak shown is from the side chain amine of W119.

that the broadening was simply due to an increased correlation time due to aggregation.

Between pH 3.0 and 2.4, a rapid drop in intensity of all cross-peaks occurred and it was not possible to recover the NMR signal by further lowering the pH, and when the pH was increased, the sample precipitated. However, by direct adjustment of the pH of a sample with a rather low protein concentration (200 μ M) to pH 1.7, it was possible to obtain a ¹⁵N HSQC spectrum (Figure 5). This spectrum retained a large degree of dispersion but exhibited approximately 30 very sharp signals, characteristic of a partially unfolded protein. When the pH was increased, the molecule refolded to give the normal pG spectrum. Unfortunately, the protein suffers from low stability at low pH, and we have thus far been unable to obtain spectra to allow assignment of this region.

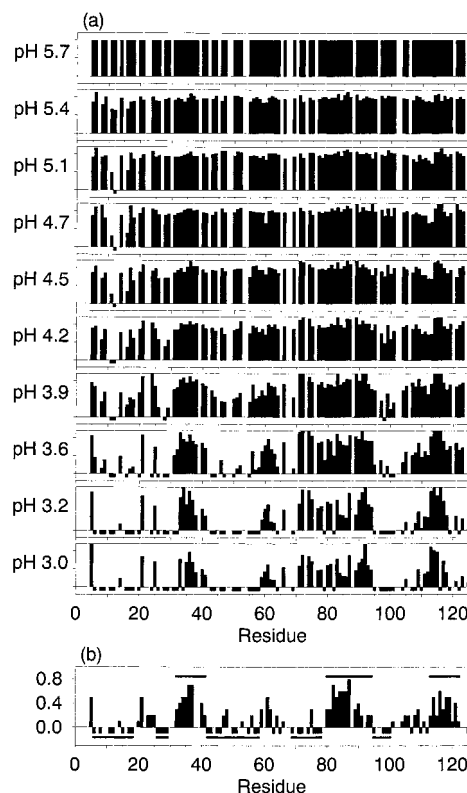


FIGURE 4: Comparison of exchange broadening when the pH is lowered in the dark and when pB is formed. (a) Variation of peak height of backbone amide ¹⁵N HSQC cross-peaks of PYP in the dark with decreasing pH, normalized to the intensity at pH 5.7. (b) Intensities of backbone amide ¹⁵N HSQC cross-peaks in the pB state, relative to the intensity in pG. The horizontal bars denote stretches mentioned in the text. In both parts of the figure, a small negative bar denotes that the peak becomes too weak to detect. A missing bar indicates that the peak cannot be represented due to ambiguity or overlap.

DISCUSSION

It remains intriguing that the views of X-ray crystallography, solution state NMR, and thermodynamic studies provide such different pictures of the pB state of PYP. Clearly, pB provides a real challenge to the abilities of these techniques to provide a full description of such a state. Such a description may not just include the concept of a single "structure", but may need to include ideas of local stability and perhaps of conformational heterogeneity.

pB Retains a Stable Core, with Destabilization around E46 and T70. In the structure of pB determined crystallographi-

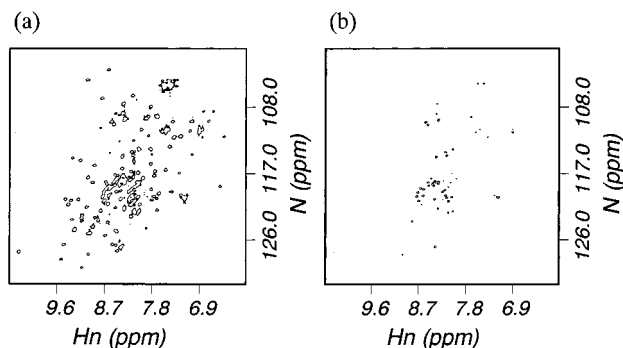


FIGURE 5: Spectrum of PYP in the dark at pH 1.7. The portion on the left is plotted at a contour level that shows all folded peaks. The portion on the right is plotted at a 10-fold higher contour level to show the peaks arising from the unfolded portion of the protein.

cally (2), there are two key changes compared to pG. First, the vinyl bond of the chromophore changes from a trans to a cis conformation, forcing the phenolic ring to undergo a large movement which results in the hydroxyl group becoming solvent-exposed and protonated. Second, the hydrogen bonds between the phenolic ring of the chromophore and the side chains of E46 and Y42 are broken. While this state is described by Genick et al. (2) as apparently a state at an energy minimum, rather than in a state of acute perturbation, it is impossible to infer from such a structure alone the effect of such a change on the stability (both local and global).

Stability changes can be probed at a residue specific level by measurements of the level of protection against amide H–D exchange (25), although such experiments are limited to those residues that show sufficient protection to remain unexchanged beyond the dead time of the experiment. The factor by which amide H–D exchange is slowed compared to that predicted for a fully unfolded peptide is termed the protection factor. The usual interpretation of the protection factor is that it is related to the fraction of the time for which the amide group is involved in a hydrogen bond. Thus, if the protection factor is x , then the hydrogen bond is formed for a fraction of the time $1 - 1/x$.

From the data presented in Figure 2, it is apparent that the residues for which the most significant loss in protection occurs are F28 (and to a lesser extent G29), E46, and T70. The loss of protection of E46 is clear evidence that the repacking of the chromophore seriously perturbs the region of the protein to which it was previously hydrogen bonded. As shown in Figure 6, the α -carbon of G29 is closely packed against one of the side chain oxygens of E46 in both pG and the crystallographically determined structure of pB, and thus, it can be understood why G29 and F28 also lose protection. In contrast, the loss of protection for residue T70 presumably arises because it is adjacent to the chromophore attachment residue, C69, and is sensitive to the perturbing effect on the protein backbone of the repacking of the chromophore. These are the only regions where the data definitely show a destabilization that leads to a very low level of residual protection, with residual protection factors of ~ 10 . For the other residues for which definite reduction in protection can be quantified, the level of residual protection remains relatively high, and with residual protection factors of ~ 1000 it is not possible from these data alone to state whether the reduction in the level of protection of these latter residues simply indicates other local stability perturba-

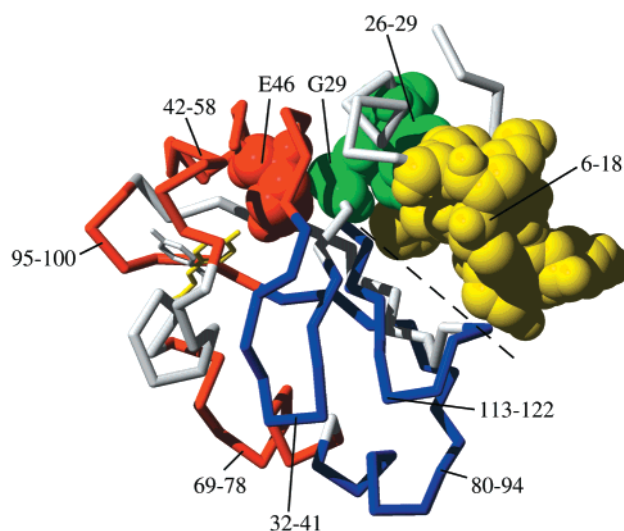


FIGURE 6: Structure of PYP in pG and in the X-ray structure of pB. The coordinates that are represented are from the structure of Genick et al. (2) (PDB entry 2pyp). At this level of representation, the coordinates of the backbone in the two conformations are indistinguishable. The chromophore is shown in yellow for pG and in white for pB. Residues 32–41, 80–94, and 113–122 are colored blue. Residues 42–58, 69–78, and 95–100 are colored red. Residues 6–18 and 26–29 are shown as space-filling diagrams and are colored yellow and green, respectively. Residue E46 (which is in contact with G29) is also shown as a space-filling diagram in red. The division between the bulk of the protein and the domain containing residues 1–28 is shown with a broken line.

tions, or perhaps an overall reduction in fold stability. Results of amide H–D exchange experiments in the pB state have previously been reported using mass spectrometry to determine the degree of H–D exchange (10). Such measurements only measure the total change in mass of the whole molecule, and therefore cannot distinguish between a locally massively increased H–D exchange rate and an overall slight drop in stability. However, the observation in the mass spectrometry data of the H–D exchange after 30 min at pH 7 of the mass equivalent to 16 extra residues compared to data collected under dark conditions is consistent with the definite observation here of 14 residues (black bars in Figure 2) for which stability drops can be measured. Although the local losses of protection observed in the data presented here still leave the residues with a substantial protection factor, the protection losses are sufficient to explain the mass spectrometry results. Thus, both data confirm the retention of a solid core of protected residues, and the NMR data are able to pinpoint two local sites of substantially reduced stability. It must be stressed that neither set of data can rule out, or prove, substantial loss of protection in residues that are only rather weakly protected in pG, due to the unavoidable dead time of these experiments.

At pH ~ 3 , PYP Displays Conformational Exchange in the Same Parts of the Molecule as pB. The changes in the UV–visible region of the absorption spectrum of PYP at low pH in the pB_{dark} state are inferred to arise from protonation of the chromophore in the absence of cis–trans isomerization (9). Such an event is also likely to disrupt the hydrogen bonding pattern in the region of E46. The reduction in the intensity of ^{15}N HSQC peaks (Figure 4), the change in the direction of movement of cross-peaks in the ^{15}N HSQC spectrum (Figure 3b), and the broadening of methyl resonances (Figure 3), all of which start to become apparent at

pH 3.9, correlate well with the transition to pB_{dark} which occurs between pH 4 and 1.5, with a p*K* of 2.8 (9). Exchange broadening effects can be significant when only a small proportion of the second form is present. For instance, pronounced effects were evident in a protein–DNA complex at only 0.1 molar equiv of added DNA (26).

We have reported previously (4) that in the pB state, 30–40% of the residues in the protein give rise to no detectable backbone amide ¹⁵N HSQC cross-peak, which was attributed to exchange broadening due to conformational exchange on a millisecond time scale. In Figure 4b, the ratios of the intensities of these cross-peaks in the pB spectrum are plotted relative to their intensity in the pG spectrum. This representation highlights the fact that there are regions of sequence where substantial cross-peak intensity is retained, notably for stretches comprising residues 32–41, 80–94, and 113–122. In contrast, there are also regions where fairly uniform cross-peak intensity is completely lost, in particular, stretches comprising residues 6–18, 26–29, 42–58, 69–78, and 95–100. These two different types of region are shown in Figure 6. In interpreting exchange broadening effects, it must be borne in mind that the effect arises from the resonance experiencing two or more environments with distinct chemical shifts. The difference in chemical shift may arise from a sequence-local effect related to changes in backbone or side chain conformation, or may arise from a change in packing of different elements of sequence against each other.

It can be seen in Figure 6 that residues 32–41, 80–94, and 113–122 are packed together and form a relatively unperturbed core. Three of the regions where cross-peak intensity is lost are colored red in Figure 6, and are closely related to the region of chromophore rearrangement. Thus, residues 69–78 include the chromophore attachment residue, C69, and residues 42–58 include the majority of the residues that have different coordinates in the X-ray structure of pB_{xtl} compared to pG. Residues 95–100 make up a loop linked to residues 42–58 via a hydrogen bond between the side chains of Y98 and R52. This hydrogen bond is broken in pB, with R52 becoming hydrogen bonded to the phenolic proton of the chromophore. In contrast, residues 6–18 and 26–29, which are colored yellow and green in Figure 6, are much more distant from the chromophore rearrangement site, and it is much more difficult to explain why they should be perturbed in pB. This apparent anomaly is discussed further below.

When the pH is lowered, the regions of PYP in which backbone amide ¹⁵N HSQC cross-peak intensity is lost are strikingly similar to those in pB (Figure 4). This is most clear in the pH range of 3.6–3.0. In terms of the regions defined above, there is a close correlation of intensity loss for the stretches of residues 6–18, 26–29, 42–58, and 95–100, but substantial intensity is retained in residues 69–78. The lack of perturbation of this latter region may be related to the fact that such a state does not involve isomerization of the chromophore vinyl bond, the chromophore attachment residue being C69. The behavior of the four well-resolved methyl signals in the one-dimensional NMR spectrum (Figure 3) shows further similarity between PYP at pH ~3.2 and pB, with three of the four peaks becoming broadened below the detection threshold, leaving a single remaining peak close to the shift of V83 H². The atoms corresponding to the three resonances that are lost are all within 7 Å of the

chromophore, whereas the V83 H² methyl group is at a distance of 16 Å.

Thus, the pH data confirm the idea that the PYP molecule can be induced into a state where a large portion of the molecule is in a state of significant conformational exchange, while retaining a well-ordered core.

Why Is the N-Terminal Region of the Molecule Perturbed? Borgstahl et al. (27) describe the PYP molecule as consisting of a central β-sheet flanked on both sides by a hydrophobic core. The major hydrophobic core includes the chromophore moiety, whereas the minor hydrophobic core is formed by the packing of the N-terminal 28-residue segment against the opposite side of the β-sheet. The minor hydrophobic core comprises residues F6, I11, L15, M18, L23, L26, and F28 in the segment of residues 1–28 and A30, W119, and F121 from the β-sheet. The interface region is rather flat, and in topological terms, the segment of residues 1–28 might be considered to form a separate subdomain of the PYP structure. H–D exchange data in the pG form (20) indicate that this region has low intrinsic stability.

It was remarked above that it is not obvious, a priori, why residues 6–18 and 26–29 [which comprise the bulk of the N-terminal 28 residues, residues 1–5 and 19–25 corresponding closely to regions with high *B* factors in the X-ray structure of pG (27) and medium to high mobility in solution (20)] are so strongly perturbed in both the pB state and the dark state of PYP at pH ~3.2. The H–D exchange data presented here provide an explanation for this apparent anomaly. As discussed above, the data show that in pB a significant drop in local stability occurs in the region near E46 when the hydrogen bond to the chromophore is broken in the pB state. The space-filling representation of Figure 6 demonstrates the close contact between E46 and G29, which explains the destabilization of G29 and F28. It then appears that this destabilization, coupled to the inherent low stability of the structure of the N-terminal 28 residues in the pG state, leads to significant perturbation of this whole N-terminal segment. Evidently, a similar effect occurs upon protonation of the chromophore in the low-pH state.

A Model for pB Involving an Equilibrium between Two States. One can consider two basic and distinct models for pB to explain the exchange broadening observed by NMR. One is that chromophore isomerization induces a state in which there is conformational heterogeneity involving exchange between a very large number of rather similar states. Such a state resembles some forms of molten globule. The second model is that the isomerization induces an equilibrium between two distinct states which themselves may, or may not, be well structured. As we discuss below, the observation of such similar exchange broadening in the low-pH-induced transition supports the second model and suggests the nature of the two states involved.

From analysis of the absorption spectra of PYP (9), the pG to pB_{dark} transition appears to be well described by a two-state transition model. In the same work, it was also shown that even within the transition region it is possible for pG to be excited into the true pB state (which has an absorption spectrum which is detectably different from that of pB_{dark}), but that the recovery is dramatically decelerated. At pH 3.2, the pG → pB_{dark} transition is approximately 30% complete, and the recovery half-time for the pB → pG process is approximately 50 s. With such a slow recovery,

it is necessary to be sure that the NMR spectra that are observed with decreasing pH do not arise simply from a mixture of molecules in the pG state and molecules that have been excited into the pB state by stray ambient light and which accumulate due to the slow recovery. With such a slow recovery at pH ~ 3.2 , this would yield a spectrum showing slow exchange characteristics. Thus, one would observe a decrease in the number pG signals with no broadening, even if the state with which it were in exchange were itself broadened. Since, for example, clear progressive broadening of the methyl signals is observed (Figure 3), this cannot be the explanation for the effects observed.

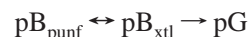
Thus, it appears that at pH ~ 3.2 the NMR spectra arise from an equilibrium between two distinct states of PYP, namely, pG and pB_{dark}. Although the solubility of the protein becomes compromised at lower pH, the spectrum obtained at pH 1.7 (Figure 5) indicates that the pB_{dark} state contains a completely unfolded region. The simplest explanation of the data shown in Figure 4 is that as the pH is lowered a two-state transition is progressively moved between a pG-like state and pB_{dark}, the interconversion being on the millisecond time scale which is quite reasonable for a partial refolding event (28). With the term "pG-like", we indicate that before the pH of the transition is reached there is at least one other detectable change in the spectrum, involving E12. However, otherwise, the spectrum is little changed, and it appears that the structure of pG is little affected, in terms of conformational order, across the pH range of 5.7–4.2. Although the pB_{dark} form is apparently partially unfolded, we may not observe very sharp signals in the spectrum of an exchanging form, because the line shape of such a spectrum is dominated by the exchange broadening and the broader line shape of the pG component. Only if the equilibrium were very substantially toward the side of the unfolded state would one start to observe the large number of very sharp signals that are observed at pH 1.7.

The ability to dissect the low-pH transition into an equilibrium between two distinct states suggests that such an equilibrium is the origin of the similar exchange broadening observed in the NMR spectrum of pB itself. This is in contrast to the alternative that the broadening arises from conformational exchange between many similar states. Furthermore, the interpretation of the pH-induced transition suggests that the two states involved are a well-ordered state and a state in which a region is totally unfolded. We will refer to this partially unfolded state as pB_{punf}. The X-ray structure of pB indicates a well-structured form, and this provides the most likely candidate for the well-structured state, which we will term pB_{xil}. The simplest explanation of all the available data is that pB in solution is in an equilibrium on a millisecond time scale between pB_{xil} and pB_{punf}.

This model is consistent with the NMR spectrum of pB. It is also consistent with the available thermodynamic data, which suggest that pB is partially unfolded, since such data would not distinguish between a pure state and an equilibrium mixture. It is also consistent with the crystallographic data with the proviso that one assumes that in the crystalline environment the ordered form is preferentially stabilized.

Evidently, the re-isomerization of the cis form of the 4-hydroxycinnamyl chromophore of PYP in the pB state is catalyzed by the "apo" protein of PYP. The evidence for this is partly based on the characteristics of PYP variants,

obtained by site-directed mutagenesis (6, 8). The isomerization is also much more rapid than would be expected for the free chromophore, the spontaneous, thermal cis to trans isomerization of 4-hydroxycinnamic acid esters being an extremely slow process, with an estimated activation energy on the order of 30 kcal/mol (H. P. M. Fennema and J. W. Verhoeven, unpublished results). If such catalysis only occurs in the rather structured environment of pB_{xil}, then one must write the recovery process as



In that case, the rate of the recovery reaction becomes sensitive not only to the relative free energy of the transition state between pB_{xil} and pG but also to the equilibrium between pB_{punf} and pB_{xil}. Such a situation closely resembles the analysis that is applicable to the rates of folding reactions via an obligatory intermediate (29) and suggests that further information can be obtained by detailed examination of the effects of denaturants and stabilizing agents on the NMR spectrum of pB and on the recovery kinetics.

In conclusion, we have shown that the nature of the ground state of PYP as the chromophore becomes protonated provides much insight into the nature of pB. It remains to be shown whether the destabilization of parts of the structure that leads to the partially unfolded form is important in exposing a binding surface involved in the molecular recognition event that constitutes the pB signaling mechanism. Alternatively, it may be important in controlling the rate of the recovery reaction, or it may simply be an unavoidable side effect of the chromophore rearrangement that truly constitutes the "signal".

ACKNOWLEDGMENT

We thank Nico Zwanenburg for help with the laser setup.

REFERENCES

1. Meyer, T. E., Yakali, E., Cusanovich, M. A., and Tollin, G. (1987) Properties of a water-soluble, yellow protein isolated from a halophilic phototrophic bacterium that has photochemical activity analogous to sensory rhodopsin, *Biochemistry* 26, 418.
2. Genick, U. K., Borgstahl, G. E. O., Ng, K., Ren, Z., Pradervand, C., Burke, P. M., Šrajcar, V., Teng, T. Y., Schildkamp, W., McRee, D. E., Moffat, K., and Getzoff, E. D. (1997) Structure of a protein photocycle intermediate by millisecond time-resolved crystallography, *Science* 275, 1471.
3. Van Brederode, M. E., Hoff, W. D., Van Stokkum, I. H. M., Groot, M. L., and Hellingwerf, K. J. (1996) Protein folding thermodynamics applied to the photocycle of the photoactive yellow protein, *Biophys. J.* 71, 365.
4. Rubinstenn, G., Vuister, G. W., Mulder, F. A. A., Düx, P. E., Boelens, R., Hellingwerf, K. J., and Kaptein, R. (1998) Structural and dynamic changes of photoactive yellow protein during its photocycle in solution, *Nat. Struct. Biol.* 5, 568.
5. Cordfunke, R., Kort, R., Pierik, A., Gobets, B., Koomen, G. J., Verhoeven, J. W., and Hellingwerf, K. J. (1998) trans/cis (Z/E) photoisomerization of the chromophore of photoactive yellow protein is not a prerequisite for the initiation of the photocycle of this photoreceptor protein, *Proc. Natl. Acad. Sci. U.S.A.* 95, 7396.
6. Devanathan, S., Genick, U. K., Canestrelli, I. L., Meyer, T. E., Cusanovich, M. A., Getzoff, E. D., and Tollin, G. (1998) New insights into the photocycle of *Ectothiorhodospira halophila* photoactive yellow protein: Photorecovery of the long-lived photobleached intermediate in the Met100Ala mutant, *Biochemistry* 37, 11563.

7. Genick, U. K., Soltis, S. M., Kuhn, P., Canestrelli, I. L., and Getzoff, E. D. (1998) Structure at 0.85 Å resolution of an early protein photocycle intermediate, *Nature* 392, 206.
8. Genick, U. K., Devanathan, S., Meyer, T. E., Canestrelli, I. L., Williams, E., Cusanovich, M. A., Tollin, G., and Getzoff, E. D. (1997) Active site mutants implicate key residues for control of color and light cycle kinetics of photoactive yellow protein, *Biochemistry* 36, 8.
9. Hoff, W. D., Van Stokkum, I. H. M., Gural, J., and Hellingwerf, K. J. (1997) Comparison of acid denaturation and light activation in the eubacterial blue-light receptor photoactive yellow protein, *Biochim. Biophys. Acta* 1322, 151.
10. Hoff, W. D., Xie, A., Van Stokkum, I. H. M., Tang, X. J., Gural, J., Kroon, A. R., and Hellingwerf, K. J. (1999) Global conformational changes upon receptor stimulation in photoactive yellow protein, *Biochemistry* 38, 1009.
11. Imamoto, Y., Kataoka, M., and Tokunaga, F. (1996) Photo-reaction cycle of photoactive yellow protein from *Ectothiorhodospira halophila* studied by low-temperature spectroscopy, *Biochemistry* 35, 14047.
12. Imamoto, Y., Mihara, K., Hisatomi, O., Kataoka, M., Tokunaga, F., Bojkova, N., and Yoshihara, K. (1997) Evidence for proton transfer from Glu-46 to the chromophore during the photocycle of photoactive yellow protein, *J. Biol. Chem.* 272, 12905.
13. Kort, R., Vonk, H., Xu, X., Hoff, W. D., Crielgaard, W., and Hellingwerf, K. J. (1996) Evidence for trans-cis isomerization of the *p*-coumaric acid chromophore as the photochemical basis of the photocycle of photoactive yellow protein, *FEBS Lett.* 382, 73.
14. Van Aalten, D. M. F., Hoff, W. D., Findlay, J. B. C., Crielgaard, W., and Hellingwerf, K. J. (1998) Concerted motions in the photoactive yellow protein, *Protein Eng.* 11, 873.
15. Xie, A., Hoff, W. D., Kroon, A. R., and Hellingwerf, K. J. (1996) Glu46 donates a proton to the 4-hydroxycinnamate anion chromophore during the photocycle of photoactive yellow protein, *Biochemistry* 35, 14671.
16. Hendriks, J., Hoff, W. D., Crielgaard, W., and Hellingwerf, K. J. (1999) Protonation deprotonation reactions triggered by photoactivation of photoactive yellow protein from *Ectothiorhodospira halophila*, *J. Biol. Chem.* 274, 17655.
17. Perman, B., Srajer, V., Ren, Z., Teng, T. Y., Pradervand, C., Ursby, T., Bourgeois, D., Schotte, F., Wulff, M., Kort, R., Hellingwerf, K., and Moffat, K. (1998) Energy transduction on the nanosecond time scale: Early structural events in a xanthopsin photocycle, *Science* 279, 1946.
18. Meyer, T. E., Tollin, G., Hazzard, J. H., and Cusanovich, M. A. (1989) Photoactive Yellow Protein From the Purple Phototrophic Bacterium, *Ectothiorhodospira halophila*: Quantum Yield of Photobleaching and Effects of Temperature, Alcohols, Glycerol, and Sucrose on Kinetics of Photobleaching and Recovery, *Biophys. J.* 56, 559.
19. Rubinstenn, G., Vuister, G. W., Zwanenburg, N., Hellingwerf, K. J., Boelens, R., and Kaptein, R. (1999) NMR experiments for the study of photointermediates: Application to the photoactive yellow protein, *J. Magn. Reson.* 137, 443.
20. Dux, P., Rubinstenn, G., Vuister, G. W., Boelens, R., Mulder, F. A. A., Hard, K., Hoff, W. D., Kroon, A. R., Crielgaard, W., Hellingwerf, K. J., and Kaptein, R. (1998) Solution structure and backbone dynamics of the photoactive yellow protein, *Biochemistry* 37, 12689.
21. Kay, L. E., Keifer, P., and Saarinen, T. J. (1992) *J. Am. Chem. Soc.* 114, 10663.
22. Delaglio, F., Grzesiek, S., Vuister, G. W., Zhu, G., Pfeifer, J., and Bax, A. (1995) *J. Biomol. NMR.* 6, 277.
23. Press, W. H., Flannery, B. P., Teukolsky, S. A., and Vetterling, W. T. (1989) *Numerical Recipes. The art of scientific computing*, Cambridge University Press, Cambridge, U.K.
24. Bai, Y., Milne, J. S., Mayne, L., and Englander, S. W. (1993) Primary structure effects on peptide group hydrogen exchange, *Proteins* 17, 75.
25. Bai, Y., Englander, J. J., Mayne, L., Milne, J. S., and Englander, S. W. (1995) Thermodynamic parameters from hydrogen exchange measurements, *Methods Enzymol.* 259, 344.
26. Dekker, N., Cox, M., Boelens, R., Verrijzer, C. P., van der Vliet, P. C., and Kaptein, R. (1993) Solution structure of the POU-specific DNA-binding domain of Oct-1, *Nature* 362, 852.
27. Borgstahl, G. E. O., Williams, D. R., and Getzoff, E. D. (1995) 1.4 angstrom structure of photoactive yellow protein, a cytosolic photoreceptor: unusual fold, active-site, and chromophore, *Biochemistry* 34, 6278.
28. Schulman, B. A., Kim, P. S., Dobson, C. M., and Redfield, C. (1997) A residue-specific NMR view of the non-cooperative unfolding of a molten globule, *Nat. Struct. Biol.* 4, 630.
29. Parker, M. J., Spencer, J., and Clarke, A. R. (1995) An integrated kinetic analysis of intermediates and transition states in protein folding reactions, *J. Mol. Biol.* 253, 771.

BI001628P